Send Orders for Reprints to reprints@benthamscience.net

CNS & Neurological Disorders - Drug Targets, XXXX, *XX*, 1-12

RESEARCH ARTICLE

Vindeburnol Induces Neuroprotection in Rat Traumatic Brain Injury *via* Adrenergic Receptor Antagonism

Mikhail Ivanov[1], Lyudmila Borets[2], Elmira Yakupova[3], Olga Riabova[2], Alexander Yurin[4], Denis Silachev[1,4,5,*] and Vadim Makarov[2]

[1]*A.N. Belozersky Research Institute of Physico-Chemical Biology, Lomonosov Moscow State University, Moscow, 119991, Russia;* [2]*Research Centre of Biotechnology of the Russian Academy of Sciences, Moscow, 119071, Russia;* [3]*Institute of Biomedical Problems of the Russian Academy of Sciences, Moscow, 123007, Russia;* [4]*Federal State Budgetary Institution "National Medical Research Center for Obstetrics, Gynecology, and Perinatology Named After Academician V.I. Kulakov", Ministry of Health of Russia, 117997, Moscow, Russia;* [5]*Translational Research Centre in Oncohaematology, Department of Cell Physiology and Metabolism, Faculty of Medicine, University of Geneva, CH-1211, Geneva, Switzerland*

ARTICLE HISTORY

Received: November 02, 2025
Revised: February 21, 2026
Accepted: March 18, 2026

DOI:
10.2174/0118715273454662260416105842

Abstract: ***Introduction/Objective*:** Traumatic Brain Injury (TBI) causes substantial neurological deficits and remains a major therapeutic challenge. This study aimed to evaluate the neuroprotective properties of Vindeburnol (VIND), a semi-synthetic derivative of vincamine, and to identify its potential molecular targets and optimal dosing regimen for post-traumatic treatment.

***Methods*:** Radioligand binding assays were used to determine VIND affinity for 22 CNS receptors, 7 ion channels, and 1 enzyme at a concentration of 10 μM. The *in vivo* neuroprotective effect was studied in a rat model of TBI induced by controlled cortical impact. VIND was administered intraperitoneally at doses of 10 or 20 mg/kg daily or every other day for 10 days. Neurological recovery was assessed using the beam-walking and limb-placement tests, and brain lesion volume was quantified by MRI on day 14.

***Results*:** VIND showed strong inhibition of radioligand binding at α1- and α2-adrenergic receptors (74% and 84.1%, respectively). *In vivo*, the most pronounced neuroprotective effect was observed at 20 mg/kg every other day, resulting in approximately a twofold reduction in lesion volume (88.7 ± 6.5 mm^3 *vs.* 179.4 ± 19.3 mm^3 in saline-treated TBI rats, $p < 0.001$) and a significant improvement in neurological outcomes. The 10 mg/kg dose showed a non-significant trend towards neuroprotection.

***Discussion*:** The neuroprotective effect of VIND is likely mediated by the inhibition of excessive adrenergic receptor activation, resulting in improved neuronal survival and functional recovery. These findings highlight adrenergic modulation as a promising therapeutic mechanism for mitigating post-traumatic brain damage.

***Conclusion*:** Vindeburnol demonstrated significant neuroprotective efficacy in a rat model of TBI and may represent a promising pharmacological candidate for post-traumatic neuroprotection.

Keywords: Traumatic brain injury, vindeburnol, adrenergic receptors, neuroprotection, CNS receptors, experimental pharmacology, neurobehavioral recovery.

1. INTRODUCTION

Traumatic Brain Injury (TBI) remains a major global public health challenge due to its high mortality and disability rates, which exceed those of all other injuries [1, 2]. Epidemiological studies highlight the scale of the problem: in 2018 alone, an estimated 69 million (95% CI 64–74 million) people worldwide suffered a TBI from all causes [1]. This high incidence, combined with serious health consequences, underlines the urgent need for targeted prevention and intervention strategies.

Currently, TBI treatment is largely supportive and focuses on critical care measures such as monitoring intracranial

* Address correspondence to this author at the A.N. Belozersky Research Institute of Physico-Chemical Biology, Lomonosov Moscow State University, Moscow, 119991, Russia; E-mail: denis.silachev@unige.ch

pressure, maintaining adequate cerebral perfusion, and optimising cerebral oxygenation [3]. These measures aim to stabilise patients and prevent secondary brain damage that may worsen outcomes. However, despite advances in acute care, these measures are often insufficient to address the long-term consequences of TBI. Many patients experience persistent cognitive deficits, motor impairments, and neuropsychiatric disorders such as depression, anxiety, and post-traumatic stress, which significantly affect their quality of life and functional independence. Therefore, the search for new therapeutic approaches to reduce the neurological consequences of TBI is a very important task for current biomedical research.

Recent advances in neuroprotective pharmacotherapy have focused on adrenergic receptor modulation. Neuroprotective effects have been demonstrated for atipamezole, an α2-adrenoceptor antagonist, in a rat model of focal cerebral ischaemia using behavioural tests [4]. Blocking adrenergic receptors (a combination of propranolol, prazosin, and atipamezole) reduced stroke volume and neurological deficit, decreased asynchronous aberrant astrocytic Ca^{2+} activities, and facilitated normalisation of extracellular ion balances in the photothrombosis mouse model [5].

One promising neuroprotective molecule is Vindeburnol (VIND) ((±)-(3α,14β)-20,21-dinoreburnamenine-14-ol; developmental codes RU24722 or BC19), a structural analogue of vincamine, a known cerebral vasodilator and alkaloid derived from Vinca minor. VIND has attracted attention for its potential therapeutic effects in various neurological conditions due to its multiple pharmacological properties, including anti-inflammatory effects and modulation of cerebral blood flow [6]. Preclinical studies have demonstrated the efficacy of VIND in several *in vivo* models of brain disease. For example, in multiple sclerosis models, VIND has shown promise in reducing neuroinflammation and demyelination, as well as promoting remyelination and functional recovery [7, 8]. In models of Alzheimer's disease, VIND reduced amyloid burden in the hippocampus and cortex, areas involved in the regulation of anxiety-like behaviour in 5x-FAD mice [8]. Recent research has also highlighted its antidepressant-like effects in models of depression-like behaviour. VIND was found to modulate monoaminergic neurotransmission and reduce stress-induced neuronal damage [6].

Several lines of indirect evidence support the idea that VIND exerts its pharmacological effects through adrenergic receptor antagonism. First, VIND has been shown to modulate dopamine metabolism and affect the electrical activity of Locus Coeruleus (LC) neurons in a manner similar to known α2-adrenergic receptor antagonists, such as yohimbine and piperoxan [9]. Second, studies in rats have demonstrated that VIND increases tyrosine hydroxylase activity and specific protein content in noradrenergic cells of the LC, implying a further role in adrenergic signalling. Notably, the activating effects of VIND on the LC were antagonised by clonidine, a well-characterised α2-adrenergic agonist, suggesting that VIND interacts with α2-receptors in a functionally distinct way [10].

Based on these findings, the present study investigates the antagonistic properties of VIND on neuronal receptors and explores its potential neuroprotective effects in a rat model of TBI.

2. MATERIALS AND METHODS

2.1. Vindeburnol Synthesis

Vindeburnol (VIND, RU24722, BC19, 1,11-diazapentacyclo- [9.6.2.02,7.08,18.015,19]nonadeca-2,4,6,8 [18]-tetraen-17-ol) was synthesized as previously described by Chen *et al*. [11] with slight modifications, and its purity was determined by High-Performance Liquid Chromatography (HPLC) analysis.

2.2. Radioligand Binding Assays *In Vitro*

The radioligand binding assays were conducted by Eurofins Discovery (France, https://www.eurofinsdiscoveryservices.com) on a fee-for-service basis. The affinity of Vindeburnol for 22 CNS receptors, 7 ion channels, and 1 enzyme was tested in radioligand binding assays at a concentration of 10 μM in DMSO solution (Eurofins, France). The experiment was carried out in accordance with the Eurofins validation standard operating procedure. All radioligand binding assays were performed in 96-well plates using binding buffer (25 mM HEPES, 100 mM NaCl, 2 mM $MgCl_2$, and 1 mM 3-[(3-cholamidopropy) dimethyl ammonio]-1-propanesulfonate (CHAPS) at pH 7.4 (NaOH)). Depending on the assay, different receptor/ion channel/enzyme sources, ligands, receptor antagonists/agonists, and time and temperature of incubation were used (Table **1**). Ligand binding was determined by filtering the assay mixture through GF/C Whatman filters (Cytiva, Marlborough, MA, USA). After washing the filters, liquid scintillation counting was performed to quantify radioactivity, except for serotonin, for which radioligand binding detection was used. The binding of the compound was calculated as the percentage inhibition of binding of a radiolabelled ligand specific to each target. The receptor binding assays were performed twice.

The binding of vindeburnol to CNS receptors was calculated as the percentage inhibition of a receptor-specific radioligand. Results showing inhibition or stimulation of less than 25% are considered non-significant and are mostly due to variability of the signal around the control value. Results showing inhibition or stimulation between 25% and 50% indicate weak to moderate effects. Results showing inhibition or stimulation of more than 50% in assays performed under basal conditions are considered significant effects of the test compounds.

2.3. Animals

For the experiment, adult male Wistar rats aged 3 months and weighing 250–300 grams were used. The animals were obtained from the animal facility of the A.N. Belozersky Institute of Physico-Chemical Biology. All animal

Table 1. Experimental protocol of radioligand binding assays *in vitro.*

Assay	Source	Ligand	Conc.	Kd	Non Specific	Incubation
Receptors						
α1 (non-selective) (antagonist radioligand)	Rat cerebral cortex	[^{3}H]prazosin	0.25 nM	0.09 nM	prazosin (0.5 μM)	60 min RT
α2 (non-selective) (antagonist radioligand)	Rat cerebral cortex	[^{3}H]RX 821002	0.5 nM	0.38 nM	(-)epinephrine (100 μM)	60 min RT
CB_1*(h)* (agonist radioligand)	Human recombinant (CHO cells)	[^{3}H]CP 55940	0.5 nM	3.5 nM	WIN 55212-2 (10 μM)	120 min 37°C
CB_2*(h)* (agonist radioligand)	Human recombinant (CHO cells)	[^{3}H]WIN 55212-2	0.8 nM	1.5 nM	WIN 55212-2 (5 μM)	120 min 37°C
D_1*(h)* (antagonist radioligand)	Human recombinant (CHO cells)	[^{3}H]SCH 23390	0.3 nM	0.2 nM	SCH 23390 (1μM)	60 min RT
D_{2S}*(h)* (antagonist radioligand)	Human recombinant (HEK-293 cells)	[^{3}H]methyl-spiperone	0.3 nM	0.15 nM	(+)butaclamol (10 μM)	60 min RT
D_{2S}*(h)* (agonist radioligand)	Human recombinant (HEK-293 cells)	[^{3}H]7-OH-D-PAT	1 nM	0.68 nM	Butaclamol (10 μM)	60 min RT
D_{2L}*(h)* (antagonist radioligand)	Human recombinant (HEK-293 cells)	[^{3}H]methyl-spiperone	0.3 nM	0.1 nM	Butaclamol (10 μM)	60 min RT
D_3*(h)* (antagonist radioligand)	Human recombinant (CHO cells)	[^{3}H]methyl-spiperone	0.3 nM	0.085 nM	(+)butaclamol (10 μM)	60 min RT
$D_{4.4}$*(h)* (antagonist radioligand)	Human recombinant (CHO cells)	[^{3}H]methyl-spiperone	0.3 nM	0.19 nM	(+)butaclamol (10 μM)	60 min RT
D_5*(h)* (antagonist radioligand)	Human recombinant (GH4 cells)	[^{3}H]SCH 23390	0.3 nM	0.25 nM	SCH 23390 (10 μM)	60 min RT
GABA (non-selective) (agonist radioligand)	Rat cerebral cortex	[^{3}H]GABA	10 nM	15 nM	GABA (100 μM)	60 min RT
$GABA_{A1}$*(h)* (α1,β2,γ2) (agonist radioligand)	Human recombinant (CHO cells)	[^{3}H]muscimol	15 nM	30 nM	Muscimol (10 μM)	120 min RT
$GABA_{B(1b)}$*(h)*(antagonist radioligand)	Human recombinant (CHO cells)	[^{3}H]CGP 54626	1 nM	1 nM	CGP 52432 (100 μM)	120 min RT
H_1*(h)* (antagonist radioligand)	Human recombinant (HEK-293 cells)	[^{3}H]pyrilamine	1 nM	1.7 nM	Pyrilamine (1 μM)	60 min RT
H_3*(h)* (agonist radioligand)	Human recombinant (CHO cells)	[^{3}H]N^{α}-Me-histamine	1 nM	0.32 nM	(R)α-Me-histamine (1 μM)	60 min RT
LPA_1*(h)* (agonist radioligand)	Human recombinant (CHO cells)	[^{3}H]LPA	2 nM	19 nM	LPA (10 μM)	90 min RT
M_5*(h)* (antagonist radioligand)	Human recombinant (CHO cells)	[^{3}H]4-DAMP	0.3 nM	0.3 nM	Atropine (1 μM)	60 min RT
N neuronal α7 *(h)* (antagonist radioligand)	Human recombinant (SH-SY5Y cells)	[^{125}I]α-bungarotoxin	0.05 nM	0.34 nM	α-bungarotoxin (1 μM)	120 min 37°C
Opioid (non-selective) (antagonist radioligand)	Rat cerebral cortex	[^{3}H]naloxone	1 nM	2.6 nM	Naloxone (1 μM)	40 min RT
Sigma (non-selective) *(h)* (agonist radioligand)	Jurkat cells (endogenous)	[^{3}H]DTG	10 nM	41 nM	Haloperidol (10 μM)	120 min RT
Serotonin (5-Hydroxytryptamine) 5- HT1 (non-selective)	Rat cerebral cortex	[^{3}H]Serotonin (5-HT)	1 nM	0.62 nM	Serotonin (5-HT) (10 μM)	60 min 25°C
Ion Channels						
BZD (central) (agonist radioligand)	Rat cerebral cortex	[^{3}H]flunitrazepam	0.4 nM	2.1 nM	Diazepam (3 μM)	60 min 4°C
AMPA (agonist radioligand)	Rat cerebral cortex	[^{3}H]AMPA	8 nM	82 nM	L-glutamate (1 mM)	60 min 4°C
Kainate (agonist radioligand)	Rat cerebral cortex	[^{3}H]kainic acid	5 nM	19 nM	L-glutamate (1 mM)	60 min 4°C
NMDA (antagonist radioligand)	Rat cerebral cortex	[^{3}H]CGP 39653	5 nM	23 nM	L-glutamate (100 μM)	60 min 4°C

(Table 1) Contd….

Assay	Source	Ligand	Conc.	Kd	Non Specific	Incubation
Glycine (strychnine-insensitive) (antagonist radioligand)	Rat cerebral cortex	[^{3}H]MDL 105,519	0.5 nM	5 nM	Glycine (1 mM)	45 min 0°C
PCP (antagonist radioligand)	Rat cerebral cortex	[^{3}H]TCP	10 nM	13 nM	MK801 (10 μM)	120 min 37°C
Cl^- channel (GABA-gated) (antagonist radioligand)	Rat cerebral cortex	[^{35}S]TBPS	3 nM	14.6 nM	Picrotoxinin (20 μM)	120 min RT
Transporters						
Norepinephrine transporter (h) (antagonist radioligand)	Human recombinant (CHO cells)	[^{3}H]nisoxetine	1 nM	2.9 nM	Desipramine (1 μM)	120 min 4°C
Dopamine transporter (h) (antagonist radioligand)	Human recombinant (CHO cells)	[^{3}H]BTCP	4 nM	4.5 nM	BTCP (10 μM)	120 min 4°C
GABA transporter (antagonist radioligand)	Rat cerebral cortex	[^{3}H]GABA (+ 10 μM isoguvacine) (+ 10 μM baclofen)	10 nM	4600 nM	GABA (1 mM)	30 min RT
Choline transporter (CHT1) *(h)* (antagonist radioligand)	Human recombinant (CHO cells)	[^{3}H]hemicholinium-3	3 nM	3.9 nM	Hemicholinium-3 (10 μM)	60 min RT
5-HT transporter *(h)* (antagonist radioligand)	Human recombinant (CHO cells)	[^{3}H]imipramine	2 nM	1.7 nM	Imipramine (10 μM)	60 min RT
Other Enzymes						
MAO-A (antagonist radioligand)	Rat cerebral cortex	[^{3}H]Ro 41-1049	10 nM	14 nM	Clorgyline (1 μM)	60 min 37°C

Abbreviations: α1–alpha-1 adrenergic receptor; α2–alpha-2 adrenergic receptor; CB_1–the type 1 cannabinoid receptor; CB_2–the type 2 cannabinoid receptor; D_1–dopamine D1 receptor; D_{2S}–the short isoform of dopamine D2 receptors; D_{2L}–long isoform of dopamine D2 receptors; D_3–dopamine D3 receptor; $D_{4.4}$–4-repeat variants of dopamine D4 receptors; D_5–dopamine D5 receptor; GABA–γ-amino butyric acid receptor; $GABA_{A1}$(α1,β2,γ2)–GABAA receptor including α1β2γ2 subunit; $GABA_B$(1b)–GABA type B receptor subunit 1 isoform X2; H_1–histamine H1 receptor; H_3–histamine H3 receptor; LPA_1–lysophosphatidic acid receptor 1; M_5–muscarinic receptor M5 subtype; N neuronal α7–α7 nicotinic acetylcholine receptor; Opioid–opioid receptor; Sigma-sigma receptor; Serotonin-serotonin receptor; BZD–benzodiazepine receptor; AMPA–α-amino-3-hydroxy-5-methyl-4-isoxazolepropri-onic acid receptor/Na+ ion channel; Kainate–Kainate receptors/tetrameric ligand-gated ion channel; NMDA–N-methyl D-aspartate receptor/ligand-gated cation channel; Glycine–glycine receptor/ligand-activated Cl− ion channel; PCP–Phencyclidine receptor; 5-HT transporter–5-Hydroxytryptamine serotonin transporter; MAO-A–Monoamine oxidase A.

procedures were approved by the Bioethics Committee of the A.N. Belozersky Institute of Physico-Chemical Biology (Protocol No. 4/23, 12 April 2023) and conducted in accordance with the Guide for the Care and Use of Laboratory Animals of the U.S. National Research Council. This study adheres to internationally accepted standards for animal research, following the 3Rs principle. The ARRIVE guidelines were employed for reporting experiments involving live animals, promoting ethical research practices.

Rats were maintained under controlled conditions, including a 12:12-hour light:dark cycle, a stable temperature of 22 ± 2°C, and unrestricted access to standard chow and drinking water. Prior to induction of TBI, animals underwent a 14-day quarantine. Standard exclusion criteria (such as pre-operative illness, abnormal behaviour, surgical complications, or failure to recover from anaesthesia) were predefined, but none of the animals met these criteria during the experiment. All animals meeting the inclusion criteria (healthy adult male Wistar rats, 250–300 grams, 3 months old) were included in the study. Standard humane endpoints (weight loss > 20%, inability to eat or drink, severe apathy, persistent seizures, self-mutilation) were predefined; no animals reached these criteria.

2.4. TBI Model

All surgical procedures were performed under inhalation anaesthesia with isoflurane (Aerrane, Baxter HealthCare Corporation, USA). Anaesthesia was induced at a concentration of 5% and maintained at 1.5–2.5% for the duration of the procedure. Body temperature was regulated using a heating pad with a rectal sensor to ensure stable thermoregulation. Additionally, the surgical site on the head was locally anaesthetised with lidocaine to minimise discomfort. The experimental model used was a modified version of focal open severe TBI in rats, based on established methods [12, 13]. Prior to surgery, the scalp of each animal was shaved, and the rat was securely immobilized in an RWD 71000 automated stereotaxic device (RWD Life Science, Sugar Land, TX 77478, USA). The scalp was disinfected with Ioprep solution, and strict aseptic techniques were maintained throughout the procedure to prevent infection. A longitudinal incision was made in the scalp to expose the skull. A trephination window with a diameter of 5 mm was carefully drilled into the skull, targeting the sensorimotor cortex region (stereotaxic coordinates relative to bregma: 2.5 mm lateral and 1.5 mm caudal). A mechanical percussion device was used to induce traumatic brain injury. This device consisted of a 50 grams weight dropped from a height of 10 cm through a hollow tube attached to a stand. The weight impacted the brain to a depth of 3 mm below the bone, ensuring the injury was localized above the dura mater. After the injury, the wound was carefully closed with a simple interrupted suture and treated with an antiseptic to promote healing and prevent infection. In the sham-operated control group, the animals underwent identical procedures, including anaesthesia, scalp incision, trephination, and suture, but were not exposed to mechanical impact.

2.5. VIND Intervention

The animals were randomly divided into five groups [1]: the TBI control group, which received 1 mL saline intraperitoneally (i.p.) daily for 10 days (n = 6) [2]; the sham-operated control group, which received 1 mL saline i.p. daily for 10 days (n = 5) [3]; the TBI + VIND 20 mg/kg daily group, which received 20 mg/kg VIND i.p. daily for 10 days, starting the day after TBI induction (n = 8) [4]; the TBI + VIND 20 mg/kg every other day group, which received 20 mg/kg VIND i.p. every other day for 10 days, starting the day after TBI induction (n = 7); and [5] the TBI + VIND 10 mg/kg every other day group, which received 10 mg/kg VIND i.p. every other day for 10 days, starting the day after TBI induction (n = 6). The experimental design is shown in Figs. (**1A-E**). Randomization was performed using the online tool Mouse-Randomization (JS) to ensure unbiased group allocation. The same animals were used consistently for behavioral and MRI analyses, and group sizes were identical for all tests. All experimental groups were coded, and investigators performing behavioural tests, MRI, and data analysis were blinded to group allocation. Only the principal investigator (Denis N. Silachev) knew the group composition to ensure correct dosing and records.

2.6. Beam Walking Test (BWT)

Neurological assessment was performed using the beam walking test, as previously described [14-16]. The BWT was performed on the 14th day after TBI. The narrowing beam is 135 cm long. The beam is designed so that the animals have a large area (5 cm wide) at the start. The width of the beam gradually decreases to 3 cm in the middle and 1.5 cm just before the resting chamber. The beam and the resting cage are positioned 50 cm above the floor. A mirror was attached to allow simultaneous observation of all four paws. The experiment was recorded with a video camera. At the start of each trial, a bright light was switched on above the starting point to encourage the rats to cross the beam. The animals were trained for three days before TBI modelling. They learned to walk on the board towards the box. For the test, each rat was placed in a dark box filled with sawdust for 5 minutes. The animal was then placed at the other end of the board and allowed to walk back on its own. Each animal underwent this test three times in succession as part of the assessment. To evaluate the neurological deficit, we counted the total number of steps, half faults (slips), and foot faults (placing the limbs on the bottom board). The deficit was scored using the following formula: Neurological deficit = ((foot faults + 0.5 × half faults) / total number of steps) × 100.

2.7. Limb-Placing Test (LPT)

The test was performed three days before the injury and again on the 7th and 14th days after the TBI to measure sensorimotor impairments. The test was based on a published protocol [17] with modifications by Jolkkonen *et al*. [4] and

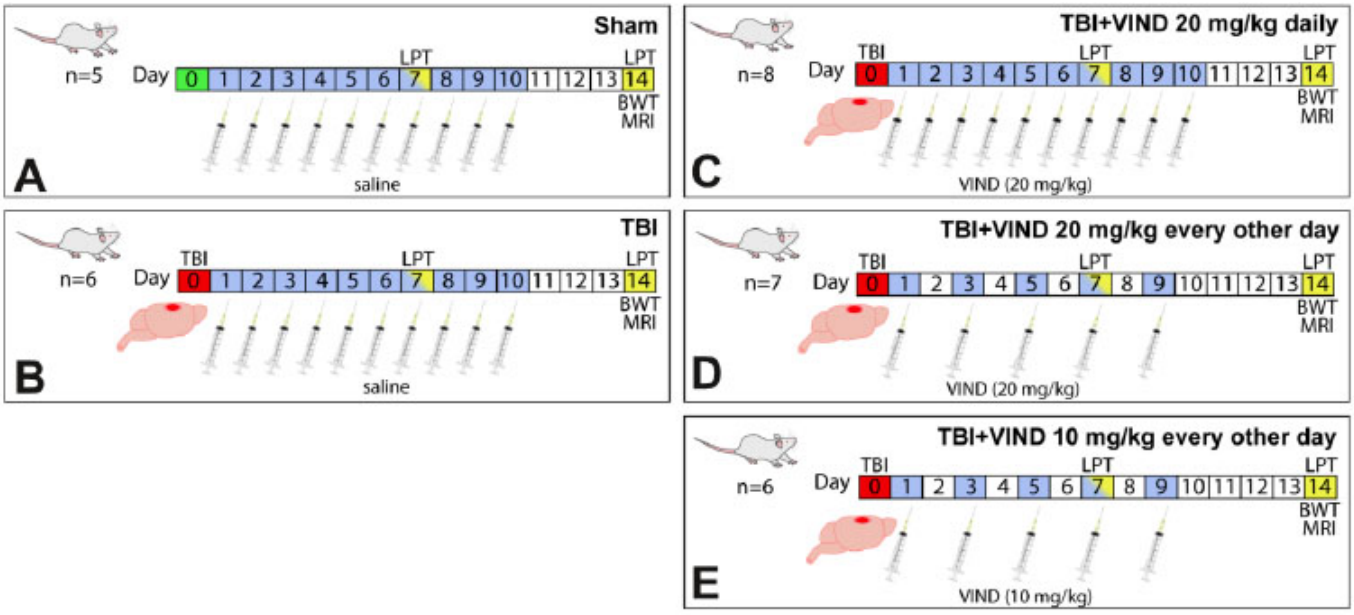

Fig. (1). Experimental design of the VIND intervention study in a TBI model. Animals were randomly assigned to five groups: (**A**) TBI + Saline, control (1 mL saline i.p. daily for 10 days; n = 6); (**B**) Sham-Operated + Saline, control (1 mL saline i.p. daily for 10 days; n = 5); (**C**) TBI + VIND 20 mg/kg daily (20 mg/kg VIND i.p. daily for 10 days post-TBI; n = 8); (**D**) TBI + VIND 20 mg/kg every other day (20 mg/kg VIND i.p. every other day for 10 days post-TBI; n = 7); and (**E**) TBI + VIND 10 mg/kg every other day (10 mg/kg VIND i.p. every other day for 10 days post-TBI; n = 6). Neurological testing timeline: On day 14 post-TBI, the Beam Walking Test (BWT) was performed to assess motor coordination and neurological deficits. Sensorimotor function was evaluated using a limb-placing test on days 7 and 14 post-TBI. On day 14 post-TBI, brain damage was assessed using a 7 Tesla MRI scanner. (*A higher resolution / colour version of this figure is available in the electronic copy of the article*).

included seven tasks assessing forelimb and hindlimb sensorimotor activity. The limb-placing test assesses an animal's ability to position its limbs correctly in response to specific sensory cues, thereby evaluating sensorimotor integration, proprioception, and limb coordination. Each task was performed on both sides to sensitively detect unilateral neurological deficits typical of focal brain injury. Both sides were assessed; however, as performance on the non-injured side remained at baseline with no detectable impairment, only the scores for the injured side are presented. The results were scored as follows: normal performance (fast and complete) – 2 points; slow (> 2 seconds) and/or incomplete performance – 1 point; failed test – 0 points.

2.8. Magnetic Resonance Imaging (MRI)

The study was conducted on day 14 after the TBI. The work was carried out on a tomograph with a magnetic field induction of 7 Tesla and a gradient system of 105 mT/m (BioSpec 70/30, Bruker, Germany). Animals were anesthetized with isoflurane (1.5%–2%) and placed in a positioning device with a stereotaxic and thermoregulation system as previously described [15].

A standard rat brain examination protocol was used, including acquisition of T2-weighted images. A linear transmitter with an inner diameter of 72 mm was used to transmit the radiofrequency signals, and a receiver coil on the surface of the rat brain was used to detect the radiofrequency signals. The following Pulse Sequences (PS) were used: RARE-PS based on a spin echo with the parameters TR = 6000 ms, TE = 63.9 ms, slice thickness 0.8 mm with a step of 0.8 mm, matrix size 256 × 384, and resolution 0.164 × 0.164 mm/pixel. The total scanning time for one animal was approximately 25 minutes. The degree of brain damage was assessed by quantitative analysis of MRI images, with calculation of the volume of the damaged brain area using ImageJ 1.52k software (National Institutes of Health image software, Bethesda, MD, USA) in mm^3.

2.9. Statistical Analysis

Statistical analysis of the quantitative data was conducted using GraphPad Prism 6 software (GraphPad Software, Boston, MA, USA). All recorded data points were included in the analysis. No animals or datasets were excluded according to the predefined criteria, as no exclusion events occurred. The normality of data distribution was assessed using the Shapiro–Wilk test. For single-time-point parameters with a normal distribution, one-way ANOVA followed by Sidak's post hoc test was used. For behavioural data collected at multiple time points (days 7 and 14) that did not meet the assumptions of normality, the Kruskal–Wallis test with Dunn's post hoc test was applied to compare differences between groups at each time point. For comparisons involving five groups of animals at two different time points, two-way ANOVA was used to analyse the LPT data. Results are expressed as mean ± SEM, with $*p < 0.05$, $**p < 0.005$, $***p < 0.0005$, $****p < 0.0001$ considered statistically significant.

3. RESULTS

3.1. *In Vitro* Pharmacology: Radioligand Binding Assays

The affinity of VIND for CNS receptors (n = 22), ion channels (n = 7), and the MAO-A enzyme was tested in pharmacological radioligand binding assays at a concentration of 10 μM (Eurofins, France). The results are presented in Fig. (**2**). Notably, VIND significantly inhibited the binding of the non-selective antagonists prazosin and RX821002 to the adrenergic receptors α1 and α2 by 74% and 84.1%, respectively. Additionally, VIND showed inhibition between 25% and 50% (indicating weak to moderate effects) at the sigma receptor (44.7%), the dopamine transporter (34.9%), MAO-A (29%), and the 5-HT transporter (27.3%). These values should be confirmed by further testing, as they fall within a range where greater inter-experimental variability may occur.

3.2. The Effect of VIND on the Volume of Brain Damage in the TBI Model

The extent of cortical damage was visualized and quantified using T2-weighted MRI (Fig. **3A**). On day 14 after TBI, pronounced hyperintense areas were detected in the ipsilateral cortex and subcortical regions of the TBI group, corresponding to zones of tissue loss, necrosis, and glial transformation within the post-traumatic cavity. In contrast, the VIND-treated groups showed a visible reduction in the hyperintense lesion area, indicating attenuation of secondary degeneration and partial preservation of cortical structure. The most prominent reduction in lesion size was observed in rats treated with VIND at 20 mg/kg every other day, in which the hyperintense region was markedly smaller, and the cortical boundaries appeared more distinct than in untreated TBI animals. Quantitative MRI analysis supported these observations, confirming the differences in lesion volumes between the groups (Fig. **3B**). The lesion volume in the TBI group was 179.4 ± 19.28 mm^3. In the TBI + VIND (20 mg/kg daily) group, the lesion volume was 165.3 ± 11.29 mm^3, while in the TBI + VIND (20 mg/kg every other day) group, it was significantly reduced to 88.7 ± 6.5 mm^3. The TBI + VIND (10 mg/kg every other day) group showed a lesion volume of 141.7 ± 12.4 mm^3. A significant reduction in lesion volume (approximately a twofold decrease) was observed in the group receiving VIND at 20 mg/kg every other day compared to the TBI group ($p < 0.001$). However, no significant reduction was observed in the groups treated with VIND at 10 mg/kg every other day or 20 mg/kg daily.

3.3. The Effect of VIND on Neurological Deficit After TBI

Neurological function and limb sensorimotor performance were assessed using the LPT on days 7 and 14 after TBI (Fig. **4A**) and BWT on day 14 (Fig. **4B**). At baseline (3 days before injury), no neurological deficits were detected in the LPT. After TBI, LPT scores decreased significantly compared with the Sham group on day 7 and remained reduced on day 14 (Fig. **4A**). Notably, on day 7, both

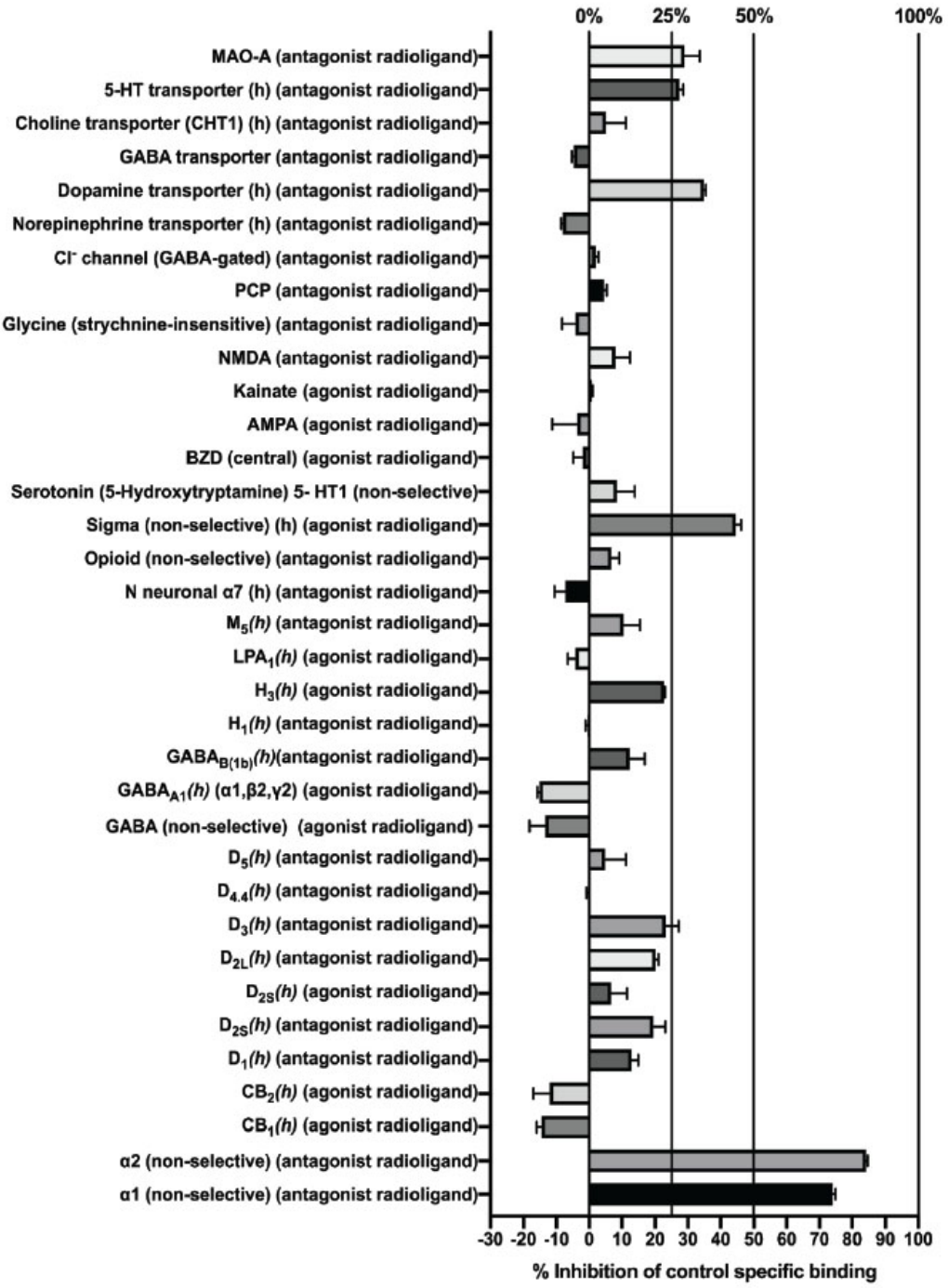

Fig. (2). *In vitro* pharmacology of Vindeburnol (VIND). Percentage inhibition of radioligand binding to 22 CNS receptors, 7 ion channels, and 1 enzyme by VIND at a concentration of 10 μM (n = 2 independent experiments, Eurofins Discovery, France). Binding was assessed in radioligand competition assays under standard SOP conditions (Table **1** for details). Results were classified according to inhibition levels: < 25% inhibition was considered non-significant (background variability), 25–50% indicated weak to moderate interaction, and > 50% indicated a significant effect. VIND showed the strongest antagonistic activity at α1-adrenergic receptors (74% inhibition) and α2-adrenergic receptors (84.1% inhibition). Moderate effects were also observed for the sigma receptor (44.7%), dopamine transporter (34.9%), MAO-A (29%), and serotonin transporter (27.3%). These findings indicate a high antagonistic affinity of VIND for adrenergic receptors, consistent with its proposed mechanism of neuroprotection in TBI. (*A higher resolution / colour version of this figure is available in the electronic copy of the article*).

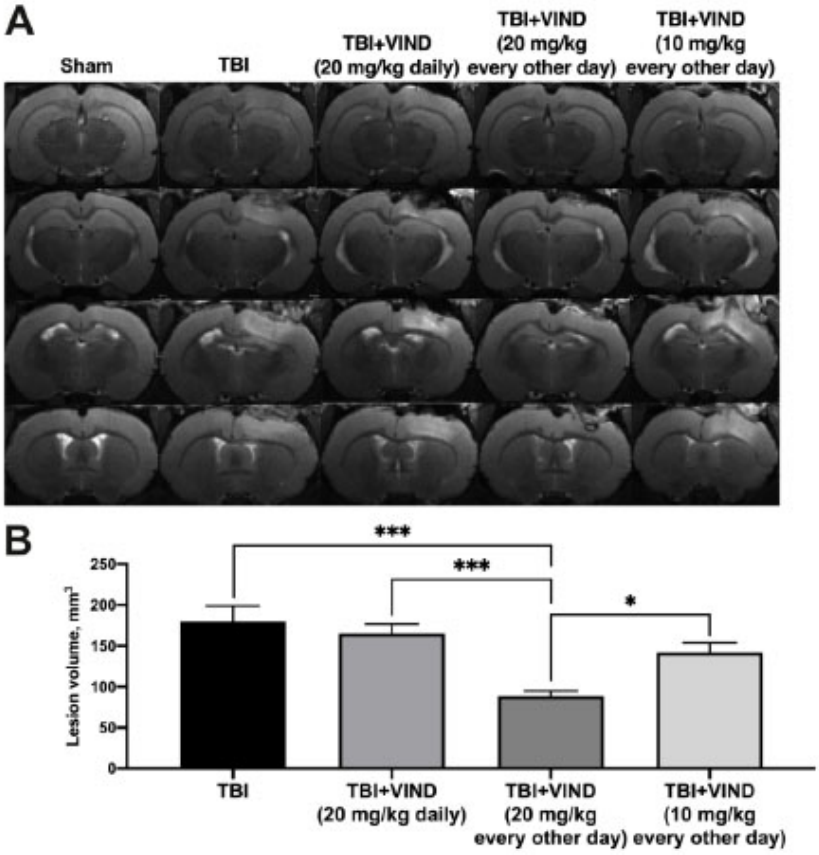

Fig. (3). Magnetic resonance imaging assessment of VIND neuroprotective effects after TBI in rats. (**A**) Representative T2-weighted coronal MRI sections of rat brains on day 14 after TBI, showing the cortical lesion area (hyperintense zone) in the ipsilateral hemisphere. A reduction in the hyperintense area is evident in the VIND-treated groups, particularly in rats receiving 20 mg/kg every other day. (**B**) Quantitative analysis of lesion volume based on MRI data. Vindeburnol administration at 20 mg/kg every other day significantly reduced lesion volume compared with untreated TBI rats ($p < 0.001$). Data are presented as mean ± SEM (n = 6–8 per group). Statistical analysis: one-way ANOVA with Sidak's multiple comparisons test, *$p < 0.05$, ***$p < 0.001$. (*A higher resolution / colour version of this figure is available in the electronic copy of the article*).

every-other-day regimens (20 and 10 mg/kg) showed improved LPT performance versus untreated TBI, whereas daily VIND did not. By day 14, the LPT continued to show a trend towards better performance in the every-other-day groups.

The BWT performed on day 14 showed a marked increase in neurological deficit in TBI rats compared with Sham animals (Fig. **4B**). Daily administration of VIND (20 mg/kg) did not improve BWT performance. In contrast, VIND administered at 20 mg/kg every other day significantly reduced the neurological deficit on day 14, producing an approximately 1.7-fold improvement compared with untreated TBI rats ($p < 0.05$). The 10 mg/kg every-other-day regimen showed a similar, but non-significant, tendency towards improvement.

4. DISCUSSION

In this study, the neuroprotective properties of VIND were demonstrated in a rat TBI model. This was reflected in both a reduction in lesion volume as determined by MRI (Fig. **3**) and an improvement in neurological status as demonstrated by LPT and BWT (Fig. **4**). A dosage of 20 mg/kg administered every other day was most effective [1]: a significant reduction in lesion volume by approximately twofold ($p < 0.0001$) [2]; a reduced significance of changes in neurological score compared to the difference between Sham and TBI groups on day 14 after TBI [3]; a decrease in neurological deficit on day 14 after TBI as demonstrated by BWT. A tendency toward decreased values of these parameters was also observed at a dosage of 10 mg/kg every other day, but no statistically significant difference was found compared to the TBI group. It should be noted that daily administration of Vindeburnol at a dose of 20 mg/kg had no neuroprotective effect. The observation that Vindeburnol 20 mg/kg administered every other day outperformed the same daily dose likely reflects schedule dependence rather than a contradiction in the dose–response relationship. In our profiling, VIND showed strong α1/α2 adrenergic antagonism, consistent with noradrenergic modulation as a key mechanism.

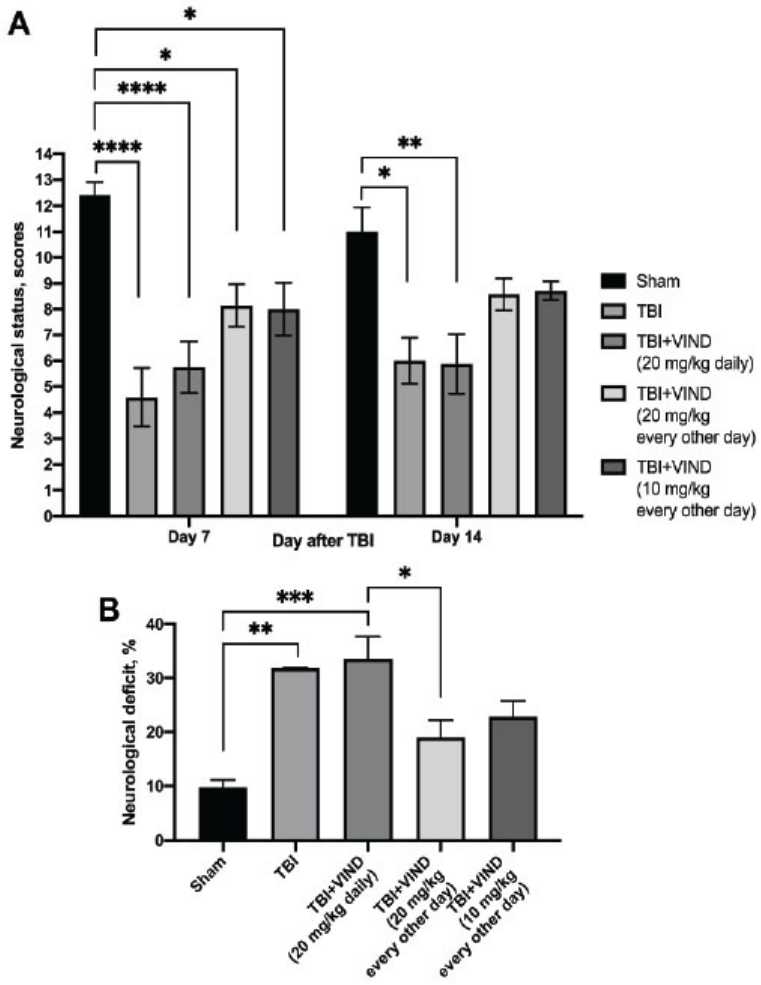

Fig. (4). Evaluation of the neuroprotective effect of VIND after induction of TBI in rats. (**A**) The effect of the different VIND administrations on neurological status as determined by the LPT test within 7 and 14 days after TBI, data are presented as mean ± SEM, *$p < 0.05$, **$p < 0.001$, ****$p < 0.0001$ (Kruskal–Wallis test); (**B**) Assessment of the severity of neurological deficit (%) using the beam-walking test at day 14 after TBI (summarized data on forelimb and hindlimb deficits in rats). Data are presented as mean ± SEM, *$p < 0.05$, **$p < 0.001$, ***$p < 0.0001$ (one-way ANOVA). (*A higher resolution / colour version of this figure is available in the electronic copy of the article*).

Sustained adrenergic perturbation can elicit compensatory adaptations that blunt the response: in humans, venous α1 blockade by terazosin diminished over 28 days despite stable plasma levels, indicating pharmacological tolerance [18]. Similarly, β-adrenergic signaling shows rapid tachyphylaxis during continuous dobutamine infusion [19], whereas intermittent infusions with drug-free intervals have been reported to avoid tolerance [20]. Frequency-dependent loss of effect is also documented for β2 agonists, where regular dosing can reduce bronchoprotective and reliever responses [21, 22]. These data support the general principle that dosing frequency and uninterrupted target engagement can determine net efficacy in adrenergic/GPCR systems. Although receptor adaptation was not directly assessed *in vivo* in this study, we hypothesize that administering the treatment every other day may limit adaptive dampening and thus preserve functional noradrenergic signalling during recovery.

In addition to its effects in traumatic brain injury, Vindeburnol has also been studied in behavioural models, where repeated administration (20 mg/kg for 21 days) alleviated depression-like symptoms and enhanced noradrenergic activity in the locus coeruleus, supporting its broader neuropsychiatric potential [6]. Recently published pharmacokinetic profiling reports a short elimination half-life for vindeburnol after intraperitoneal administration (t1/2 ≈ 2.4 hours), indicating a transient exposure profile after each injection. While this supports the feasibility of "pulsed" target engagement, the superior efficacy of every-other-day dosing in our study likely reflects pharmacodynamic factors, such as receptor-system adaptation and timing of recovery processes, rather than exposure duration alone [23]. Historically, RU24722 (vindeburnol), administered in a pulsed schedule after ischaemia (*e.g.*, 15 minutes, 10, 24, and 34 hours after ischaemia), has improved EEG and metabolic recovery, suggesting that inter-

mittent exposure may be beneficial in acute brain injury [24, 25]. Combining these data with our results, we propose that alternating daily administration of VIND after TBI may better preserve adrenergic signalling windows for recovery while avoiding receptor adaptation, thereby outperforming daily administration. These observations emphasise the need for further studies, including measurement of vindeburnol levels in blood and brain, assessment of potential receptor adaptation with repeated dosing, and systematic testing of different administration schedules in larger animal cohorts.

VIND has previously been shown to enhance antioxidant defences (glutathione peroxidase and reductase) and increase the expression of tyrosine hydroxylase and Noradrenaline (NA) in the Locus Coeruleus (LC), thereby supporting neuroprotection in models of multiple sclerosis [7, 8]. Based on these observations and our radioligand data showing robust α_1/α_2 antagonism, we propose that VIND confers neuroprotection after TBI *via* converging mechanisms. VIND belongs to the eburnamine–vincamine alkaloid family; however, its receptor interaction profile may differ from that of vincamine. While vincamine is mainly discussed in the context of cerebrovascular, antioxidant, and ion channel-related mechanisms, our screening revealed a pronounced interaction of VIND with α1- and α2-adrenergic receptor binding sites, which warrants direct head-to-head profiling of vincamine under identical conditions [26]. In the radioligand screen, VIND produced marked inhibition of radioligand binding at non-selective α1 and α2 adrenergic receptor sites in rat cortical membrane preparations (74% and 84.1% inhibition at 10 μM, respectively). However, the current binding assays do not distinguish between presynaptic autoreceptors and postsynaptic receptor populations, and functional characterisation will be required to determine the net impact on noradrenaline signalling. First, functional antagonism of α_2-autoreceptors may facilitate activity-dependent NA release from LC projections, promoting plasticity and attenuating microglial inflammation. There is growing evidence that noradrenergic signalling plays a central role in regulating microglial activation states, thereby influencing neuroinflammation, synaptic remodeling, and functional recovery after brain injury. Noradrenaline acting *via* β_2-adrenergic receptors suppresses the release of proinflammatory cytokines and shifts microglia towards a neuroprotective phenotype, while modulation of α_2-receptors alters the availability of noradrenaline and further influences the balance between deleterious and reparative microglial responses [4, 27-29]. Second, adrenergic receptor antagonism can accelerate the normalization of extracellular K^+ and shorten the recovery of spontaneous activity after injury, reducing susceptibility to Cortical Spreading Depolarization (CSD), a process mechanistically linked to astrocytic α_1-dependent Ca^{2+} signalling and ion homeostasis. Adrenergic receptor antagonism accelerated the normalization of extracellular K^+, leading to a faster recovery of neural activity in the photothrombosis model of focal cerebral ischaemia [5, 30]. Third, under pathophysiological conditions, α_1-adrenergic blockade may attenuate the excessive vasoconstrictive drive of the sympathetic nervous system in cerebral vessels, reducing vascular resistance, improving regional cerebral blood flow, and supporting perfusion of peri-lesional or penumbral tissue at risk of secondary ischaemic damage [31]. These pathways are also consistent with clinically relevant observations that CSDs impose a significant metabolic burden on the injured brain through massive ion fluxes, glutamate release, and cerebral blood flow disturbances. Recurrent CSDs not only exacerbate energy loss and oxidative stress but also increase the area of secondary injury in both stroke and TBI patients, where their occurrence has been associated with poorer neurological outcomes and increased lesion growth [32-34]. Taken together, these data provide a conclusive explanation for why alternating daily VIND treatment performed better than daily dosing in our study: intermittent α_1/α_2 blockade preserves beneficial NA-mediated plasticity, avoids receptor adaptation, promotes stabilisation of astrocyte–neuronal potassium homeostasis, and supports penumbral perfusion, whereas continuous daily dosing risks desensitisation of α_1/α_2 receptors.

LIMITATIONS

This study has several limitations that should be acknowledged. The observation period was limited to 14 days after traumatic brain injury, which did not allow assessment of long-term structural and functional recovery. The pharmacokinetic properties and brain distribution of vindeburnol were not evaluated, preventing precise interpretation of its dose–response relationship and optimal treatment window. The experiments were conducted only in adult male Wistar rats, which may limit the generalization of the results to other species, strains, or females. The proposed mechanism of action, involving antagonism at α_1 and α_2 adrenergic receptors, was inferred from *in vitro* receptor-binding assays and requires further experimental confirmation using specific pharmacological and molecular approaches. Future research should address these limitations by extending the observation period, including both sexes and other animal models, characterizing pharmacokinetic parameters, and clarifying the intracellular pathways involved in vindeburnol-mediated neuroprotection.

CONCLUSION

Our study shows that Vindeburnol exerts a significant neuroprotective effect in a rat model of traumatic brain injury. The most pronounced benefits were observed with alternate-day administration of 20 mg/kg for 10 days, resulting in reduced lesion volume in brain tissue and improved neurological outcomes. Mechanistically, these effects are likely related to the strong antagonistic activity of vindeburnol at α_1- and α_2-adrenergic receptors, indicating that adrenergic modulation is a promising therapeutic strategy to attenuate secondary damage after TBI.

AUTHORS' CONTRIBUTIONS

The authors confirm their contributions to the paper as follows: MI: Performed the rat experiments; OR: Vinde-

burnol synthesis; AY: Conducted neurological testing; LB: Vindeburnol synthesis, interpretation of results, edited the manuscript; EY: Analysis and interpretation of results, preparation of the figures and writing of the original draft; DS: Study conception, design and supervized, interpretation of results, review and editing of the manuscript, supervised the study; MV: Study conception, design and supervision. All the authors have reviewed the results and approved the final version of the manuscript.

LIST OF ABBREVIATIONS

BWT	=	Beam Walking Test
LC	=	Locus Coeruleus
LPT	=	Limb-Placing Test
MRI	=	Magnetic Resonance Imaging
NA	=	Noradrenaline
VIND	=	Vindeburnol

ETHICS APPROVAL AND CONSENT TO PARTICIPATE

All animal procedures were approved by the Bioethics Committee of the A.N. Belozersky Institute of Physico-Chemical Biology (Protocol No. 4/23, 12 April 2023).

HUMAN AND ANIMAL RIGHTS

The study was conducted in accordance with the Guide for the Care and Use of Laboratory Animals of the U.S. National Research Council. This study adheres to internationally accepted standards for animal research, following the 3Rs principle. The ARRIVE guidelines were employed for reporting experiments involving live animals, promoting ethical research practices.

CONSENT FOR PUBLICATION

Not applicable.

AVAILABILITY OF DATA AND MATERIALS

The datasets used and analyzed during the current study are available from the corresponding authors upon reasonable request.

FUNDING

M.I., E.Y., A.Y., and D.S. conducted this work under the state assignment of Lomonosov Moscow State University.

CONFLICT OF INTEREST

The authors declare no conflict of interest, financial or otherwise.

ACKNOWLEDGEMENTS

Declared none.

REFERENCES

[1] Dewan MC, Rattani A, Gupta S, *et al.* Estimating the global incidence of traumatic brain injury. J Neurosurg 2019; 130(4): 1080-97. http://dx.doi.org/10.3171/2017.10.JNS17352 PMID: 29701556

[2] Guan B, Anderson DB, Chen L, Feng S, Zhou H. Global, regional and national burden of traumatic brain injury and spinal cord injury, 1990–2019: A systematic analysis for the Global Burden of Disease Study 2019. BMJ Open 2023; 13(10): e075049. http://dx.doi.org/10.1136/bmjopen-2023-075049 PMID: 37802626

[3] Chen C, Peng C, Hu Z, Ge L. Effects of bone marrow mesenchymal stromal cells-derived therapies for experimental traumatic brain injury: A meta-analysis. Heliyon 2024; 10(3): e25050. http://dx.doi.org/10.1016/j.heliyon.2024.e25050 PMID: 38322864

[4] Jolkkonen J, Puurunen K, Rantakömi S, Härkönen A, Haapalinna A, Sivenius J. Behavioral effects of the α2-adrenoceptor antagonist, atipamezole, after focal cerebral ischemia in rats. Eur J Pharmacol 2000; 400(2-3): 211-9. http://dx.doi.org/10.1016/S0014-2999(00)00409-X PMID: 10988336

[5] Monai H, Wang X, Yahagi K, *et al.* Adrenergic receptor antagonism induces neuroprotection and facilitates recovery from acute ischemic stroke. Proc Natl Acad Sci USA 2019; 116(22): 11010-9. http://dx.doi.org/10.1073/pnas.1817347116 PMID: 31097598

[6] Zubkov E, Riabova O, Zorkina Y, *et al.* Antidepressant-like effect of the eburnamine-type molecule vindeburnol in rat and mouse models of ultrasound-induced depression. ACS Chem Neurosci 2024; 15(3): 560-71. http://dx.doi.org/10.1021/acschemneuro.3c00590 PMID: 38216514

[7] Markovich MA, Valeryevna ZM, Dmitrievna SL. The activity of antioxidant enzymes and the expression of their genes in the rat brain after injecting of vindeburnol in the multiple sclerosis model. Eurasian Union Sci 2020; 3(3(72)): 8-11. http://dx.doi.org/10.31618/ESU.2413-9335.2020.3.72.638

[8] Polak PE, Kalinin S, Braun D, Sharp A, Lin SX, Feinstein DL. The vincamine derivative vindeburnol provides benefit in a mouse model of multiple sclerosis: Effects on the Locus coeruleus. J Neurochem 2012; 121(2): 206-16. http://dx.doi.org/10.1111/j.1471-4159.2012.07673.x PMID: 22288774

[9] Quintin L, Hilaire G, Pujol JF. Variations in 3,4-dihydroxyphenylacetic acid concentration are correlated to single cell firing changes in the rat locus coeruleus. Neuroscience 1986; 18(4): 889-99. http://dx.doi.org/10.1016/0306-4522(86)90107-7 PMID: 2876399

[10] Labatut R, Richard F, Milne B, Quintin L, Lecestre D, Pujol JF. Long-term effects of RU24722 on tyrosine hydroxylase of the rat brain. J Neurochem 1988; 51(5): 1367-74. http://dx.doi.org/10.1111/j.1471-4159.1988.tb01099.x PMID: 2902195

[11] Chen X, Yu L, Wang H, Zhang W, Tang P, Chen F. Stereoselective total synthesis of (±)-vindeburnol and (±)-16-*epi*-vindeburnol. Chem Commun 2021; 57(88): 11669-72. http://dx.doi.org/10.1039/D1CC04980A PMID: 34672312

[12] Isaev NK, Novikova SV, Stelmashook EV, *et al.* Mitochondria-targeted plastoquinone antioxidant SkQR1 decreases trauma-induced neurological deficit in rat. Biochemistry 2012; 77(9): 996-9. http://dx.doi.org/10.1134/S0006297912090052 PMID: 23157258

[13] Fournier ML, Clément T, Aussudre J, Plesnila N, Obenaus A, Badaut J. Contusion rodent model of traumatic brain injury: Controlled cortical impact. Wound Regeneration. New York: Humana 2021; pp. 49-65. http://dx.doi.org/10.1007/978-1-0716-0845-6_6

[14] Schallert T, Woodlee M, Fleming S. Disentangling multiple types of recovery from brain injury. In: Krieglstein J, Klumpp S, Eds. Pharmacology of Cerebral Ischemia. Stuttgart: Medpharm Scientific Publishers 2002; pp. 201-16.

[15] Silachev DN, Uchevatkin AA, Pirogov YA, Zorov DB, Isaev NK. Comparative evaluation of two methods for studies of experimental focal ischemia: Magnetic resonance tomography and triphenyl-

tetrazoleum detection of brain injuries. Bull Exp Biol Med 2009; 147(2): 269-72.
http://dx.doi.org/10.1007/s10517-009-0489-z PMID: 19513437

[16] Yakupova E, Bocharnikov A, Fedulova K, Babenko V, Silachev D, Plotnikov E. Changes in bioenergetics and neuroprotective properties of mesenchymal stromal cells after lps treatment. BIOCELL 2024; 48(12): 1827-34.
http://dx.doi.org/10.32604/biocell.2024.058496

[17] Cheng F, Yan B, Liao P, *et al.* Ischemic stroke and the biological hallmarks of aging. Aging Dis 2024; 16(5): 2908-36.
http://dx.doi.org/10.14336/AD.2024.1059 PMID: 40789569

[18] Vincent J, Dachman W, Blaschke TF, Hoffman BB. Pharmacological tolerance to alpha 1-adrenergic receptor antagonism mediated by terazosin in humans. J Clin Invest 1992; 90(5): 1763-8.
http://dx.doi.org/10.1172/JCI116050 PMID: 1358918

[19] Unverferth DV, Blanford M, Kates RE, Leier CV. Tolerance to dobutamine after a 72 hour continuous infusion. Am J Med 1980; 69(2): 262-6.
http://dx.doi.org/10.1016/0002-9343(80)90387-3 PMID: 7405947

[20] Erlemeier HH, Kupper W, Bleifeld W. Intermittent infusion of dobutamine in the therapy of severe congestive heart failure- long-term effects and lack of tolerance. Cardiovasc Drugs Ther 1992; 6(4): 391-8.
http://dx.doi.org/10.1007/BF00054187 PMID: 1520649

[21] Harvey JE, Tattersfield AE. Airway response to salbutamol: Effect of regular salbutamol inhalations in normal, atopic, and asthmatic subjects. Thorax 1982; 37(4): 280-7.
http://dx.doi.org/10.1136/thx.37.4.280 PMID: 7112457

[22] Cockcroft DW, Davis BE, Swystun VA, Marciniuk DD. Tolerance to the bronchoprotective effect of β2 -agonists: Comparison of the enantiomers of salbutamol with racemic salbutamol and placebo. J Allergy Clin Immunol 1999; 103(6): 1049-53.
http://dx.doi.org/10.1016/S0091-6749(99)70178-8 PMID: 10359885

[23] Tsedilin A, Borets L, Riabova O, Kazakova E, Tafeenko V, Makarov V. Determination of alkaloid-inspired molecule vinpeburnol in rabbit plasma by UPLC–HRMS and its application to pharmacokinetic studies and preliminary metabolite identification. J Pharm Biomed Anal 2024; 239: 115917.
http://dx.doi.org/10.1016/j.jpba.2023.115917 PMID: 38101239

[24] Formento ML, Barzaghi F, Mantegazza P. Energy metabolism in the conscious gerbil during recirculation following transient ischemia: Effects of RU 24722 and vincamine. Drug Dev Res 1988; 13(1): 81-8.
http://dx.doi.org/10.1002/ddr.430130108

[25] Barzaghi F, Dragonetti M, Formento ML, Boissier JR. Effects of the new eburnamenine derivative RU 24722 on EEG recovery and cerebral energy metabolism after complete ischemia. Arzneimittelforschung 1985; 35(2): 472-7.
PMID: 4039569

[26] Ren Y, DeRose K, Li L, Gallucci JC, Yu J, Douglas Kinghorn A. Vincamine, from an antioxidant and a cerebral vasodilator to its anticancer potential. Bioorg Med Chem 2023; 92: 117439.
http://dx.doi.org/10.1016/j.bmc.2023.117439 PMID: 37579526

[27] Heneka MT, Nadrigny F, Regen T, *et al.* Locus ceruleus controls Alzheimer's disease pathology by modulating microglial functions through norepinephrine. Proc Natl Acad Sci USA 2010; 107(13): 6058-63.
http://dx.doi.org/10.1073/pnas.0909586107 PMID: 20231476

[28] Sugama S, Takenouchi T, Hashimoto M, Ohata H, Takenaka Y, Kakinuma Y. Stress-induced microglial activation occurs through β-adrenergic receptor: Noradrenaline as a key neurotransmitter in microglial activation. J Neuroinflammation 2019; 16(1): 266.
http://dx.doi.org/10.1186/s12974-019-1632-z PMID: 31847911

[29] Zou HL, Li J, Zhou JL, Yi X, Cao S. Effects of norepinephrine on microglial neuroinflammation and neuropathic pain. Ibrain 2021; 7(4): 309-17.
http://dx.doi.org/10.1002/ibra.12001 PMID: 37786561

[30] Wahis J, Holt MG. Astrocytes, noradrenaline, α1-adrenoreceptors, and neuromodulation: Evidence and unanswered questions. Front Cell Neurosci 2021; 15: 645691.
http://dx.doi.org/10.3389/fncel.2021.645691 PMID: 33716677

[31] Purkayastha S, Raven P. The functional role of the alpha-1 adrenergic receptors in cerebral blood flow regulation. Indian J Pharmacol 2011; 43(5): 502-6.
http://dx.doi.org/10.4103/0253-7613.84950 PMID: 22021989

[32] Schoknecht K, Kikhia M, Lemale CL, *et al.* The role of spreading depolarizations and electrographic seizures in early injury progression of the rat photothrombosis stroke model. J Cereb Blood Flow Metab 2021; 41(2): 413-30.
http://dx.doi.org/10.1177/0271678X20915801 PMID: 32241203

[33] Soldozy S, Sharifi KA, Desai B, *et al.* Cortical spreading depression in the setting of traumatic brain injury. World Neurosurg 2020; 134: 50-7.
http://dx.doi.org/10.1016/j.wneu.2019.10.048 PMID: 31655239

[34] Zhao HT, Tuohy MC, Chow D, *et al.* Neurovascular dynamics of repeated cortical spreading depolarizations after acute brain injury. Cell Rep 2021; 37(1): 109794.
http://dx.doi.org/10.1016/j.celrep.2021.109794 PMID: 34610299